

A search for super-imposed oscillations to the primordial power spectrum in Planck and SPT-3G 2018 data

Akhil Antony,^{1,2,*} Fabio Finelli,^{3,4,†} Dhiraj Kumar Hazra,^{5,6,3,‡} Daniela Paoletti,^{3,4,§} and Arman Shafieloo^{7,8,¶}

¹*Asia Pacific Center for Theoretical Physics, Pohang, 37673, Republic of Korea*

²*Department of Physics, POSTECH, Pohang, 37673, Republic of Korea*

³*INAF/OAS Bologna, Osservatorio di Astrofisica e Scienza dello Spazio, Area della ricerca CNR-INAF, via Gobetti 101, I-40129 Bologna, Italy*

⁴*INFN, Sezione di Bologna, via Irnerio 46, 40126 Bologna, Italy*

⁵*The Institute of Mathematical Sciences, HBNI, CIT Campus, Chennai 600113, India*

⁶*Homi Bhabha National Institute, Training School Complex, Anushakti Nagar, Mumbai 400085, India*

⁷*Korea Astronomy and Space Science Institute, Daejeon 34055, Korea*

⁸*Korea University of Science and Technology, Daejeon 34113, Korea*

(Dated: March 29, 2024)

We search for super-imposed oscillations linearly or logarithmically spaced in Fourier wavenumbers in Planck and South Pole Telescope (SPT-3G) 2018 temperature and polarization data. The SPT-3G temperature and polarization data provide a new window to test these oscillations at high multipoles beyond the Planck angular resolution and sensitivity. We consider both models with a constant and a Gaussian modulated amplitude, which correspond to three and four additional parameters beyond power-law primordial power spectrum for the templates considered, respectively. We find that each of the four models considered can provide an improved fit to Planck data, consistently with previous findings, and to SPT-3G data, always compared to Λ CDM. For a constant amplitude of the superimposed oscillations, we find tighter constraints on the amplitude of the oscillations from the combined Planck/SPT-3G data set than in each individual data sets. When the ranges of parameters which provide a better fit to Planck and SPT-3G data overlap, as in the case of Gaussian modulated oscillations, we find a larger $\Delta\chi^2$ - 17 (-16) for logarithmic (linear) oscillations - in a combined Planck/SPT-3G data set than in each individual data sets. These findings will be further tested with upcoming CMB temperature and polarization measurements at high multipoles provided by ongoing ground experiments.

PACS numbers: 98.80.Cq

I. INTRODUCTION

The power spectrum of primordial scalar fluctuations is being tested by multiple cosmological probes at different scales and redshifts. A power law spectrum embedded in the six parameters Λ CDM model is a good fit to Planck cosmic microwave background (CMB) anisotropy data, which currently has the lion's share of the constraining power among different cosmological observables within the range $\sim [0.001, 0.1] \text{ Mpc}^{-1}$. However, there are certain deviations from a power law spectrum which are still allowed by the current precision and angular resolution of Planck 2018 data [1]. Some of these deviations lead to an improved fit with a $\Delta\chi^2 \sim -[10 - 15]$ compared to a power-law spectrum, although the extra parameters beyond the amplitude A_s and the spectral index n_s penalize these models from a Bayesian point of view [1].

Oscillations linear or logarithmic in wavenumber super-imposed to the primordial spectrum are among

the deviations from a power-law with deeper theoretical foundations and with a higher $\Delta\chi^2$ for Planck data at the same time. Non-vacuum initial vacuum states for quantum fluctuations [2], resonant models including periodic oscillations in the potential [3] as axion monodromy [4] are among the mechanisms which generate super-imposed oscillations. For these reasons these models have become a workhorse for exploration with CMB anisotropy data [1, 5–8], LSS [9–12] and a benchmark for future CMB experiments [13, 14], as well as for future and ongoing galaxy surveys [15–18]. See [19–31] for other searches of primordial features in CMB data.

CMB polarization anisotropies should be a refined test for primordial features, given the sharpness of the polarization transfer functions compared to those in temperature [32]. Whereas Planck remains the main full sky data set until LiteBIRD [33], better data at higher resolution from ground experimentes such as Atacama Cosmology Telescope (ACT) [34] and South Pole Telescope (SPT) [35] are already in the public domain. The high degree of consistency between Planck and SPT-3G data has been discussed in [35]. We therefore explore oscillations linear and logarithmically spaced in k with a constant and a Gaussian modulated amplitude with Planck [36] and, for the first time, with SPT-3G 2018 data [35], as well with their combination [37]

This paper is structured as follows. After the intro-

* akhilantony@imsc.res.in

† fabio.finelli@inaf.it

‡ dhiraj@imsc.res.in

§ daniela.paoletti@inaf.it

¶ shafieloo@kasi.re.kr

duction, in Section 2 we describe the four models chosen as representative for super-imposed oscillations, the data sets used and the sampling methodology. In Section 3, we describe our results and we conclude in Section 4.

II. METHODOLOGY

In this paper, we investigate the effect of sinusoidal oscillations in the primordial power spectrum which are periodic on linear or logarithmic scales. In our study, we further examine two class of models: one where the oscillations span the entire observable range of wavenumbers (k), and another where the oscillations are localized. In the latter case, these oscillations undergo damping on both sides of a central peak. In total, we analyse four models in this study: linear and logarithmic oscillations, with constant amplitude and Gaussian modulated amplitude, as can be seen in Fig. 1

A. Models and Priors

We consider the following templates for global oscillations:

$$P_{\text{global}}^{\text{lin}}(k) = P_0(k) \left[1 + \alpha \cos \left(\omega \frac{k}{k_*} + \phi \right) \right] \quad (1)$$

$$P_{\text{global}}^{\text{log}}(k) = P_0(k) \left[1 + \alpha \cos \left(\omega \ln \frac{k}{k_*} + \phi \right) \right] \quad (2)$$

These oscillations have an amplitude α , frequency ω and a phase ϕ varying in the range $[0, 2\pi]$. Here $P_0(k)$ is the Standard Model power spectrum given as $A_s (k/k_*)^{n_s-1}$ where $k_* = 0.05 \text{ Mpc}^{-1}$.

The most general localised oscillation models extending Eqs. 1, 2:

$$P_{\text{local}}^{\text{lin}}(k) = P_0(k) \left[1 + \alpha \cos \left(\omega \frac{k}{k_*} + \phi \right) e^{-\frac{\beta^2 (k-\mu)^2}{2k_*^2}} \right] \quad (3)$$

$$P_{\text{local}}^{\text{log}}(k) = P_0(k) \left[1 + \alpha \cos \left(\omega \ln \frac{k}{k_*} + \phi \right) e^{-\frac{\beta^2 (k-\mu)^2}{2k_*^2}} \right] \quad (4)$$

contain five extra parameters, including the center μ and the width β of the Gaussian envelope. Since sampling such large parameter volume is a complex task, in this paper we mostly consider a lower dimensional space by fixing the phase in such a way that the peak of the Gaussian is located at a maximum of the oscillations $\phi = -\omega\mu/k_*$ ($\phi = -\omega \ln(\mu/k_*)$) for the linear (logarithmic) case. Fixing the phase in this way has the advantage of having just one more additional parameter compared to the templates with constant amplitude in Eqs. 1, 2, an important

aspect in sampling such a complex parameter space, and the disadvantage of a phase dependent on the frequency and peak position.

The prior ranges for the primary parameters are listed in Table I. Note that the priors chosen for global oscillations are the same adopted for logarithmic oscillation in [1].

	α	$\log_{10} \omega$	μ	β	$\phi/(2\pi)$
Linear	[0, 0.5]	[0,2.1]	-	-	[0,1]
Log	[0, 0.5]	[0,2.1]	-	-	[0,1]
Damped Linear	[0, 0.3]	[0.3, 1.7]	[0.001, 0.175]	[0,10]	-
Damped Log	[0, 0.3]	[1.0,1.8]	[0.001, 0.175]	[0,10]	-

TABLE I. Prior table

B. Datasets and Samplers

Our analyses in this paper are based only on CMB data. We work with 3 combinations of datasets, namely Planck (P18TP), SPT-3G (SPT3G) and combined P18TP and SPT-3G (P18TP+SPT3G).

We use Planck 2018 release temperature and polarization likelihoods [36]. Following the primordial feature analysis of Planck [1], we do not consider Planck lensing likelihood. Differently from the Planck analysis for features [1], we restrict ourselves to binned data, but all foreground and calibration nuisance parameters are allowed to vary along with their recommended priors [36]. In this paper we consider Plik binned data since the SPT-3G data are provided in a binned format, and we will not be able to jointly explore the high frequency oscillations domain allowed by unbinned Planck data anyway.

For SPT-3G 2018 data, we use temperature, polarization auto and their cross correlation data from 90, 150 and 220 GHz channels [38] [35]. When we use SPT only likelihood for analysis, in order to break the degeneracy between the amplitude and optical depth, we use the optical depth prior from Planck 2018 baseline analysis, $\tau = 0.054 \pm 0.074$, as recommended in [35]. Here too we allow the default nuisance parameters to vary.

The consistency and complementarity of Planck 2018 and SPT-3G 2018 data is shown in Fig. 2.

Given the lack of publicly available covariance between Planck and SPT-3G data, we consider as baseline a conservative combined Planck/SPT-3G data set in which there is no-overlap in multipoles between the two datasets. In gluing the two data sets, we follow SPT-3G release [35], where it has been discussed that SPT-3G data have smaller uncertainties than Planck above multipole $\ell = 2000$ for TT, $\ell = 1400$ for TE and $\ell = 1000$ for EE. Following that, we use a truncated version of Planck Plik TTTEEE likelihood with TT in the range $\ell = 30 - 2000$, TE in $\ell = 30 - 1400$ and EE in $\ell = 30 - 1000$. Therefore, in this combined data set, we use TT from $\ell = 2000$, TE from $\ell = 1400$ and EE from

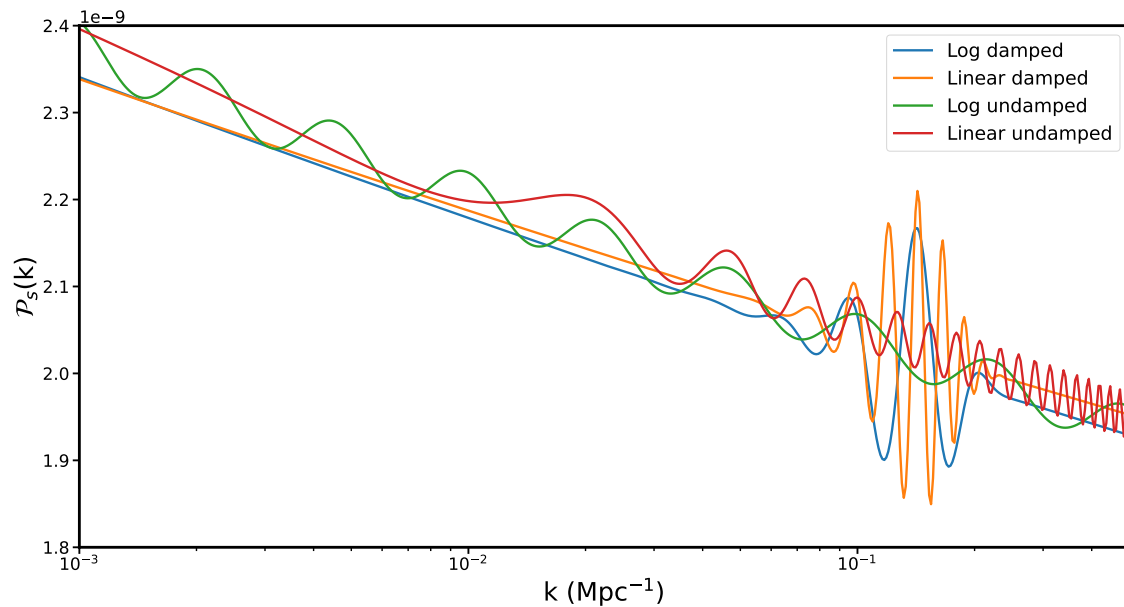


FIG. 1. Primordial curvature power spectra for the four templates considered (corresponding to the best fit values obtained from Planck + SPT analysis used as a baseline in this paper)

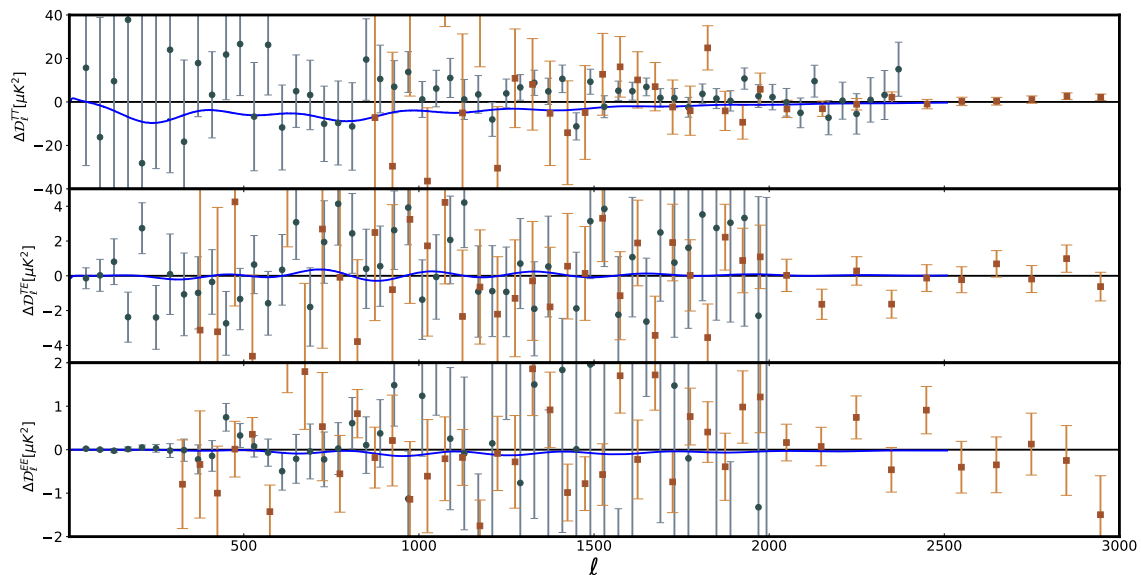


FIG. 2. Planck (black) and SPT-3G TT, TE, EE (orange) binned residuals to the Planck 2018 TP Λ CDM best-fit. The relative difference of the Λ CDM bestfit to SPT-3G data plus Planck 2018 measurement of τ with respect to the Planck 2018 TP Λ CDM bestfit is also shown for comparison (blue line).

Models	$\Delta\chi_{\text{P18}}^2$	$\ln B_{\text{P18}}$	$\Delta\chi_{\text{SPT}}^2$	$\ln B_{\text{SPT}}$	$\Delta\chi_{\text{P18+SPT}}^2$	$\ln B_{\text{P18+SPT}}$
Lin undamped	-10.7	-2.3 ± 0.4	-0.2	-2.5 ± 0.4	-9.5	-2.1 ± 0.3
Log undamped	-10.4	-3.3 ± 0.4	-11.6	-1.4 ± 0.4	-5.1	-0.8 ± 0.4
Lin damped	-13.0	-1.5 ± 0.4	-6.8	-0.8 ± 0.4	-15.8	1.0 ± 0.4
Log damped	-9.9	-1.2 ± 0.4	-14.2	-0.76 ± 0.4	-17.1	1.68 ± 0.4

TABLE II. The table illustrates improvement in fit to the data and Bayesian evidence obtained by the templates with respect to the power law primordial power spectrum. We have studied the templates, both independently and jointly, against Planck and SPT dataset. In all cases we get a good improvement in fit to the data with respect to power law power spectrum. We also find a moderate preference for damped models over the power-law power spectrum in terms of Bayesian evidence.

$\ell = 1000$ for SPT-3G data. Note that with this conservative choice the multipole $10^3 \lesssim \ell \lesssim 2 \times 10^3$ are tested by Planck in TT and by SPT-3G in EE. Although we consider this conservative choice as our baseline combination, we also perform some tests by using a combination of the full Planck and truncated SPT-3G data sets as well as another combination in which Planck likelihoods are cut as above and only SPT-3G temperature data are cut below $\ell = 2000$.

Given the multi-modal nature of posteriors, Markov Chain Monte Carlo (MCMC) is not expected to be effective in capturing parameter space. We use, therefore, Polychord [39] sampler for nested sampling of param-

eter spaces and for the computation of the Bayes factors. We use $n_{\text{live}} = 1000$ for Planck and SPT3G separately, and $n_{\text{live}} = 2000$ when we consider combined data sets. In settling for live points related to combined analysis, we compared MCMC results with Polychord for baseline model ($\Lambda\text{CDM} + \text{power law}$). For $n_{\text{live}} = 2000$ parameter posteriors obtained from Polychord converge to MCMC posteriors.

In obtaining best-fits, we use BOBYQA minimizer [40]. We identify the samples from the Polychord chains corresponding to likelihood peaks and we obtain local minima by BOBYQA around those peaks.

III. RESULTS

Results for Planck, SPT-3G and the baseline combination of Planck and SPT-3G data are presented in Table II.

We first discuss the results obtained for the undamped templates as given in Eqs. 1, 2. We find a very good agreement with the results in [1] when using Planck 2018 unbinned data and nuisance/foreground parameters fixed to the ΛCDM bestfits: both templates lead to an improvement $\Delta\chi_{\text{P18}}^2 \sim -10.5$. A very good agreement is also found with [41], where alternative Planck likelihoods have been used. With SPT-3G 2018 and the Planck prior on τ , we find a prominent peak in the posterior for $\log_{10} \omega \simeq 1.55$ with $\Delta\chi_{\text{SPT}}^2 \sim -11.6$ for logarithmic oscillations, whereas we find a negligible improvement in the SPT fit for linear oscillations, always compared to ΛCDM . For SPT3G data, we find that a contribution to this improvement comes from fitting logarithmic oscillations in the range $1000 \lesssim \ell \lesssim 2000$. For these global oscillation models, the posteriors peak at different frequency for Planck and SPT-3G 2018 data. For the Planck + SPT3G data set, we find a $\chi_{\text{P18+SPT}}^2 \sim -10$ (-5) for linear (logarithmic) undamped oscillations.

As is clear from Fig. 3, this combined Planck + SPT3G data constrain the amplitude of these oscillations in a tighter way compared to the individual data sets. We obtain $\alpha \lesssim 0.018$ ($\alpha \lesssim 0.016$) at 95 % CL from Planck plus SPT-3G for linear (logarithmic) oscillations, which improve on the corresponding Planck 95 % CL constraint

$\alpha \lesssim 0.029$ ($\alpha \lesssim 0.039$). These results demonstrate the power of the complementarity between Planck and SPT-3G in constraining models beyond ΛCDM . None of the two models are statistically preferred over the ΛCDM for any data set considered.

Following Eqs. 3, 4 we analyzed damped templates. The triangle plots for the damped linear and logarithmic template corresponding to all three datasets are provided in Fig. 4. We find that the Gaussian modulated linear oscillations provide a larger improvement in the fit to Planck data ($\Delta\chi_{\text{P18}}^2 \sim -13$) than Gaussian modulated logarithmic oscillations ($\Delta\chi_{\text{P18}}^2 \sim -10$). For SPT-3G data, the opposite occurs, i.e. Gaussian modulated logarithmic oscillations provide a better fit compared to linear oscillations (-14 vs -7). For a Gaussian modulated amplitude, we find prominent peaks at $\ln \omega_{\text{log}} \sim 1.55$ and at $\ln \omega_{\text{lin}} \sim 1.1$ for the SPT-3G data set (plus the Planck 2018 measurement for τ). The peak in the frequency for modulated linear oscillations found in SPT-3G 2018 lies very close to the one found in Planck 2018 data: this is an interesting result, also in light of the different systematics which potentially affect Planck and SPT data. These oscillations do not correspond exactly to oscillations in SPT-3G EE data found by Gaussian regression in [42]. Both models with damped oscillations with Planck plus SPT-3G data show a moderate preference with respect to ΛCDM for the priors chosen. [43]. Since the ranges of parameters which provide a better fit independently to Planck and SPT-3G data overlap for modulated oscillations, we find a larger $\Delta\chi^2$ in the combined Planck plus

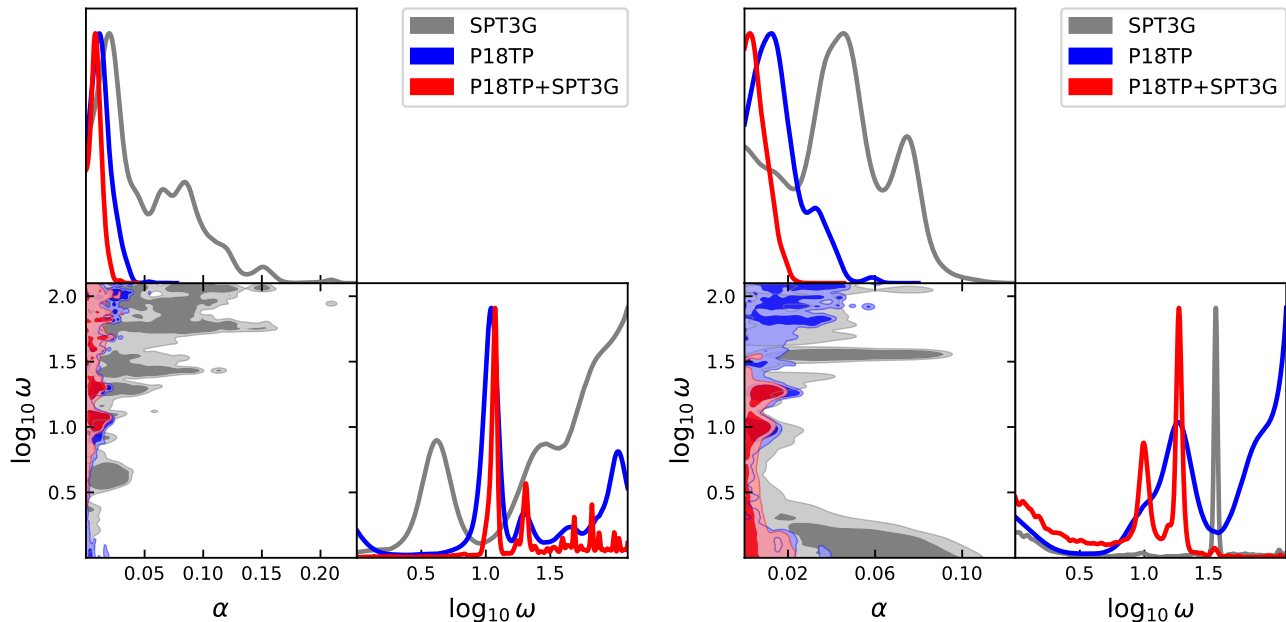


FIG. 3. Undamped power spectrum templates: Here we present the marginalised posterior distribution for amplitude and frequency of linear (on the left) and logarithmic templates (on the right) present in Eqs 1, 2. We study the templates using Planck (P18TP), SPT (SPT3G) data individually and also with a non overlapping combination of both dataset (P18TP + SPT3G).

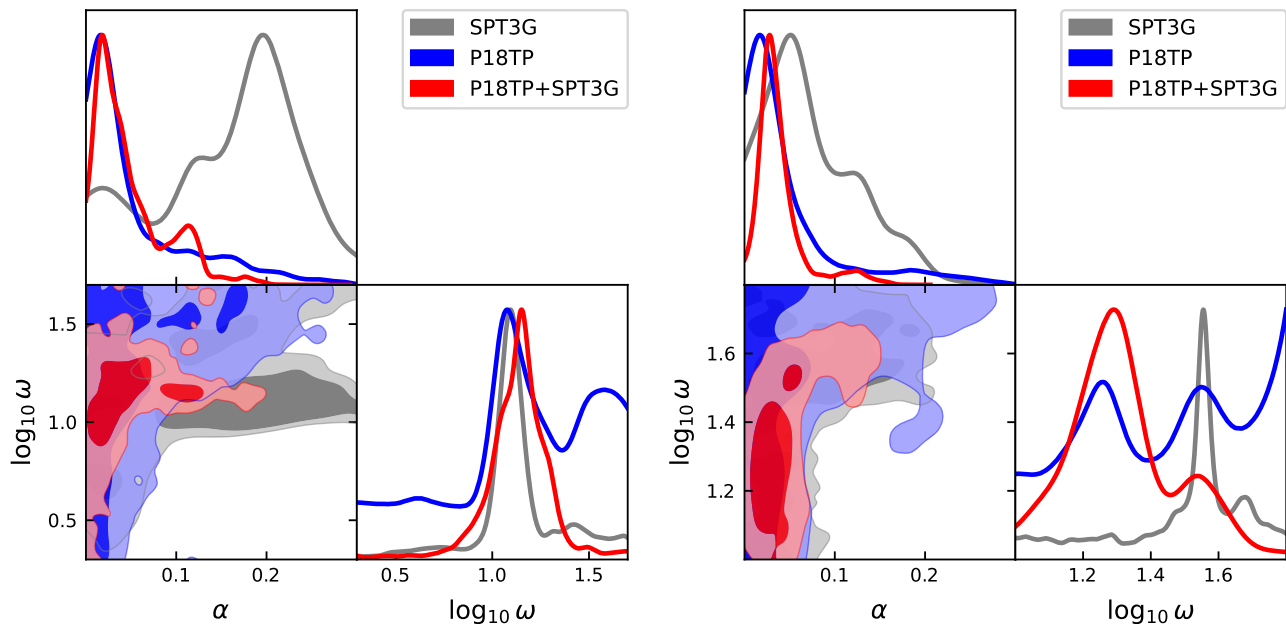


FIG. 4. Damped power spectrum templates: Here we present the marginalised posterior distribution for amplitude and frequency of linear (on the left) and logarithmic templates (on the right) present in Eqs 3, 4. We study the templates using Planck (P18TP), SPT (SPT3G) data individually and also with a non overlapping combination of both dataset (P18TP + SPT3G).

SPT-3G data set, up to the maximum $\Delta\chi^2 \sim -17(-16)$ for modulated logarithmic (linear) oscillations.

In Fig. 5 we compare the relative differences of the

Planck 2018 TP bestfits for the four models considered with respect to the corresponding Planck 2018 TP Λ CDM bestfit with the Plik TT, TE, EE binned residu-

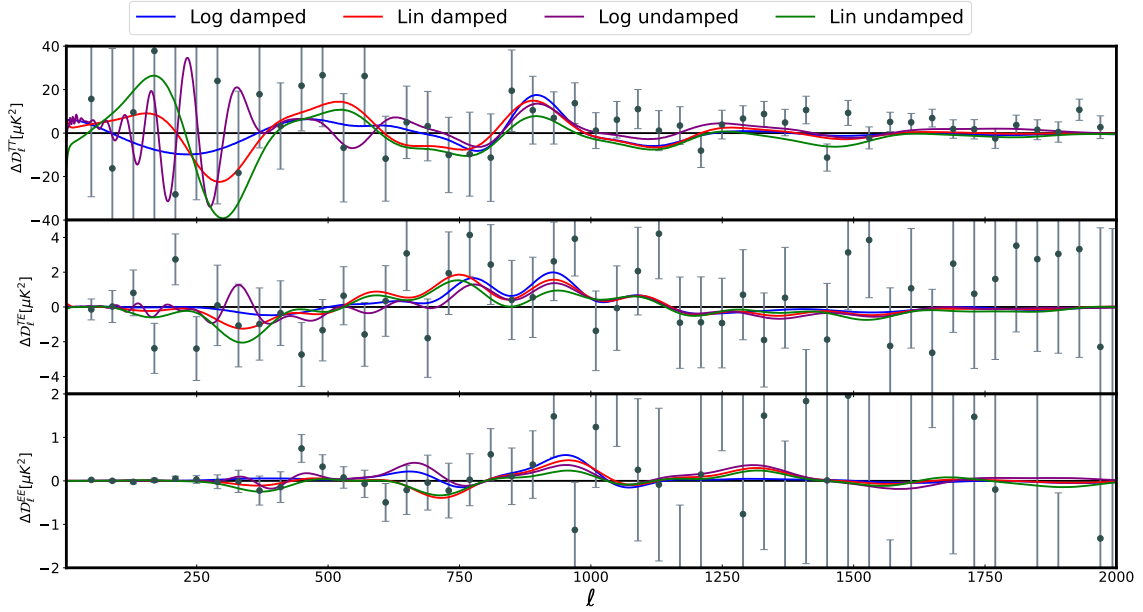


FIG. 5. Relative differences of the Planck 2018 TP bestfits for the four models considered with respect to the corresponding Planck 2018 TP Λ CDM bestfit (see legends for the colors). Plik TT, TE, EE binned residuals (black data points) to the Planck 2018 TP Λ CDM best-fit are also plotted for comparison.

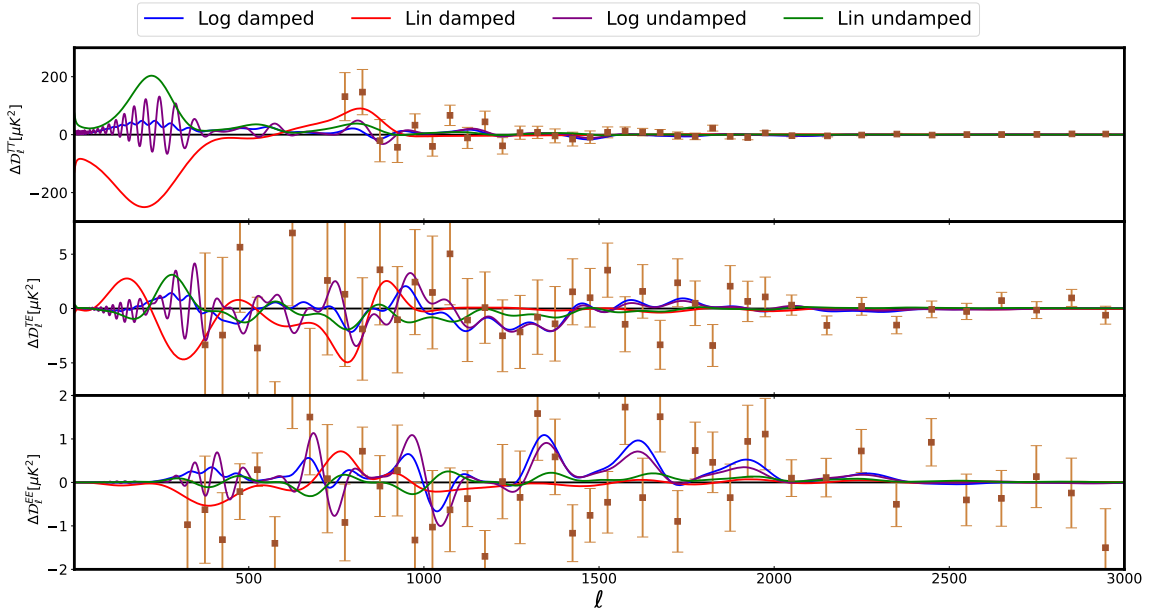


FIG. 6. Relative differences of bestfits to the SPT-3G plus Planck 2018 measurement of τ for the four models considered with respect to the corresponding SPT-3G Λ CDM bestfit (see legends for the colors). SPT-3G TT, TE, EE binned residuals (orange data points) to the SPT-3G Λ CDM best-fit are also plotted for comparison.

als. In Figs. 6 and 7 we repeat this plot for SPT-3G and the baseline Planck plus SPT-3G combination, respectively. In Fig. 8 instead we highlight the change of the

bestfits for global logarithmic oscillations and local linear oscillations induced by the combination with SPT-3G data.

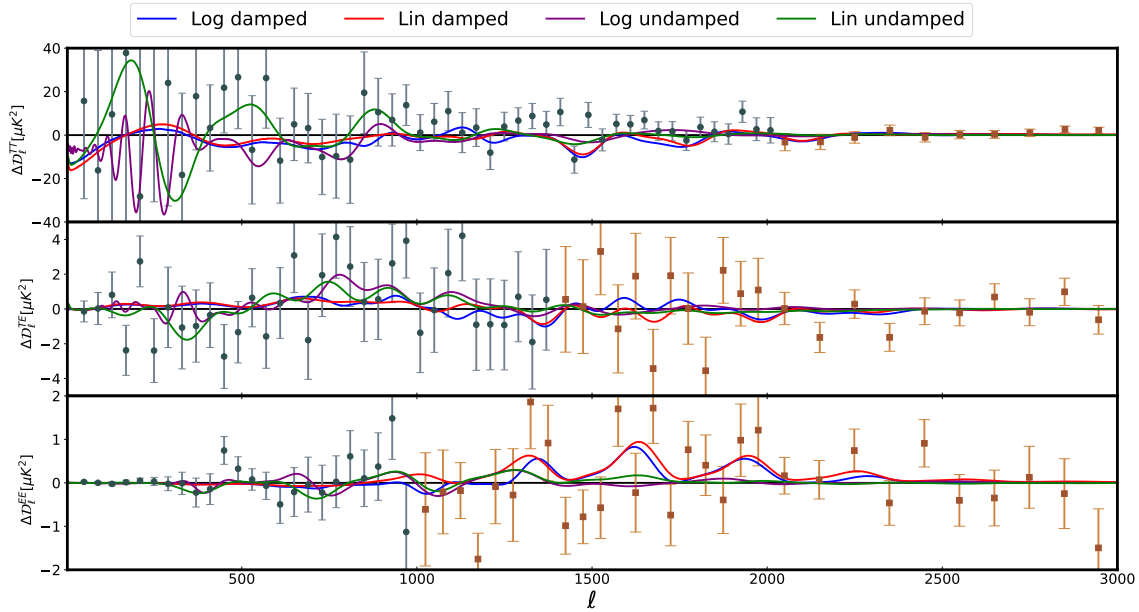


FIG. 7. Relative differences of the Planck 2018 + SPT-3G TP bestfits for the four models considered with respect to the corresponding Planck 2018 + SPT-3G TP Λ CDM bestfit (see legends for the colors). Planck Plik (black data points) + SPT-3G (orange data points) TT, TE, EE binned residuals to the Planck 2018 + SPT-3G TP Λ CDM best-fit are also plotted for comparison.

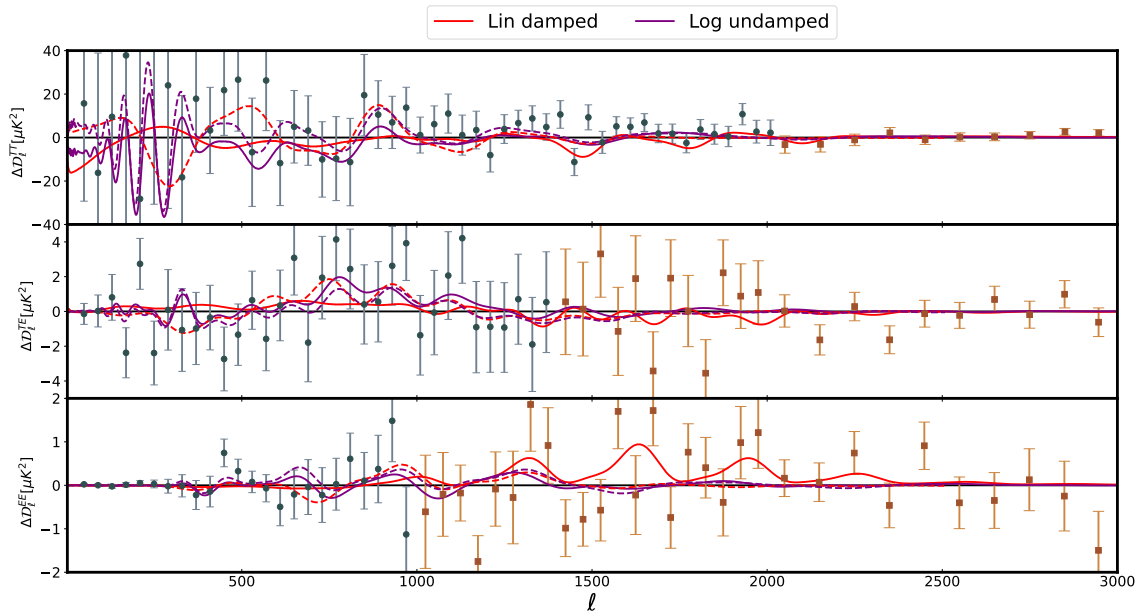


FIG. 8. Comparison of best-fits to Planck 2018 + SPT-3G (solid) to Planck 2018 bestfits (dashed) for linear localized (red) and logarithmic global oscillations (purple). Planck Plik (black data points) + SPT-3G (orange data points) TT, TE, EE binned residuals to the Planck 2018 + SPT-3G TP Λ CDM best-fit for the baseline data combination are also plotted for comparison.

We have also tested the impact of different ways of combining Planck and SPT-3G likelihoods. In Fig. 9, we

compare the posterior probabilities for the parameters of modulated logarithmic oscillations obtained by our con-

servative baseline with other two alternative combinations, i.e. a combination of the full Planck and truncated SPT-3G data sets and another combination in which only SPT-3G temperature data are cut below $\ell = 2000$

Although broadly consistent, Fig. 9 shows how posteriors differ between different combinations and how these different combinations potentially lead to tighter constraints. In particular, one alternative baseline highlights the frequency around $\ln \omega_{\log} \sim 1.55$ which improves the fit of the intermediate SPT-3G TE, EE multipoles which are cut in our baseline data combination.

IV. CONCLUSIONS

We have searched for super-imposed oscillations linearly or logarithmically spaced in Fourier wavenumbers in Planck and SPT-3G 2018 temperature and polarization data. SPT-3G angular resolution and sensitivity in polarization can test primordial features at higher multipoles beyond Planck measurements. SPT-3G 2018 temperature and polarization data [35] lead to Λ CDM parameters very consistent with Planck and can be therefore used in combination with Planck to provide a precision test for models beyond Λ CDM such as those including features in the primordial power spectrum. See [35, 44, 45] for other studies of models beyond Λ CDM with SPT-3G data.

In this analysis we use SPT-3G public (binned) data. We therefore use also Planck binned 2018 data, differently from the search for features performed in Ref. [1]. We use polychord [39] as a sampler given the multimodality of the resulting posterior distributions and we allow for variation of the foreground and nuisance parameters.

For Planck, we find results consistent with those obtained in [1] for oscillations with a constant amplitude, which produce a quite similar improvement in the fit compared to Λ CDM. When these oscillations have a Gaussian modulation, linear and logarithmic oscillations produce ~ -13 and ~ -11 as improvement in $\Delta\chi^2$, respectively.

We have tested these models with primordial oscillations with SPT-3G 2018 data for the first time. For SPT-3G 2018 data, we have found that all the models studied here improve the fit compared to Λ CDM, although are not statistically preferred over the Λ CDM. As happens for Λ CDM cosmology [35], SPT-3G is less constraining than Planck 2018 data. Our analysis shows that the frequencies preferred by SPT-3G 2018 data do not coincide with those preferred by Planck 2018 data when the amplitude of the super-imposed oscillations is constant. However, for a Gaussian modulated amplitude, we find prominent peaks at $\log_{10} \omega_{\log} \sim 1.6$ and at $\log_{10} \omega_{\text{lin}} \sim 1.1$. The peak in the frequency for modulated linear oscillations found in SPT-3G 2018 lies very close to the found in Planck 2018 data. In particular, we find that super-imposed logarithmic oscillations lead to $\Delta\chi^2 \sim -12$, and

when Gaussian modulated to $\Delta\chi^2 \sim -14$. These oscillations do not correspond exactly to oscillations in SPT-3G EE data found by Gaussian regression in [42] [46].

We have therefore constrained these models with the combination of Planck and SPT-3G data for the first time. Since a covariance between Planck and SPT-3G data is not available, we consider the main combined data set in which we cut Planck (SPT) above (below) the multipoles at which the Planck S/N is reached by SPT as stated in [35] and described in section II. This conservative procedure which enforces just one measurement for each multipole bin should overcome the issue of potentially double counting information with a full Planck and SPT-3G combination without a covariance matrix between the two experiments. By adopting this combination, we find that SPT-3G high- ℓ polarization data play an important role for all the models studied.

We find that superimposed oscillations with a constant amplitude do not improve the fit and are tighter constrained by Planck+SPT-3G 2018 compared to Planck 2018 data. When the ranges of parameters which provide a better fit independently to Planck and SPT-3G data overlap, we find a larger $\Delta\chi^2$ in the combined Planck SPT-3G data set, up to the maximum $\Delta\chi^2 \sim -17$ for modulated logarithmic oscillations.

Our findings could be extended to higher frequencies with data which are either unbinned or have a smaller binning and will be further tested with upcoming CMB temperature and polarization measurements at high multipoles by ongoing and future ground experiments, such as ACT, SPT, Simons Observatory [47] and CMB-S4 [48].

ACKNOWLEDGMENTS

The authors acknowledge the use of computational resources at the Institute of Mathematical Science's High Performance Computing facility [Nandadevi] and of CNAF HPC cluster in Bologna. FF and DKH would like to thank Karim Benabed and Silvia Galli for discussions on SPT-3G 2018 likelihood. AA is supported by an appointment to the JRG Program at the Asia Pacific Center for Theoretical Physics through the Science and Technology Promotion Fund and Lottery Fund of the Korean Government, and was also supported by the Korean Local Governments in Gyeongsangbuk-do Province and Pohang City. AA also acknowledges support from the NRF of Korea (Grant No. NRF-2022R1F1A1061590) funded by the Korean Government (MSIT). AA, FF, DKH acknowledge travel support through the India-Italy "RELIC - Reconstructing Early and Late events In Cosmology" mobility program. FF would like to thank IMSc for warm hospitality for the December 2022 visit when this work started. FF, DP acknowledge financial support from the contract by the agreement n. 2020-9-HH.0 ASI-UniRM2 "Partecipazione italiana alla fase A della missione LiteBIRD". FF, DKH, DP acknowledge financial support from Progetti di Astrofisica Fondamentale INAF

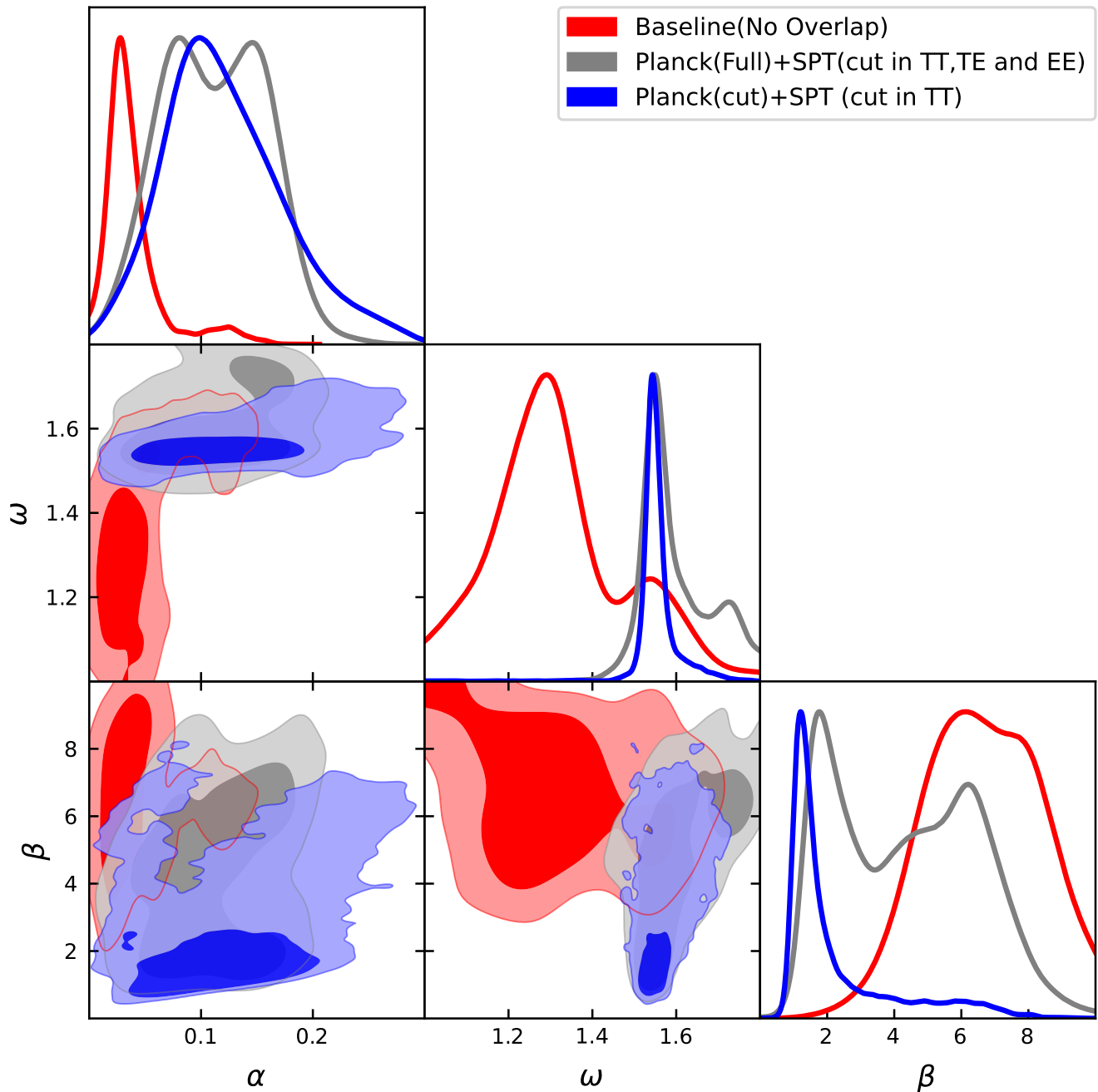


FIG. 9. Here we plot the triangular plot for the damped logarithmic model parameters analysed with different combination of Planck and SPT likelihoods. In red, we have the non overlapping (in both temperature and polarisation) combination of Planck and SPT datasets. In gray we plot the results from analysis of an uncut Planck likelihood and cut SPT (as discussed in III). Blue contours corresponds to the results from a combined likelihoods of Planck (cut as discussed in III) and SPT (cut only in TT).

2023. DKH would like to acknowledge the support from the Indo-French Centre for the Promotion of Advanced Research – CEFIPRA grant no. 6704-4. AS would like to acknowledge the support by National Research Founda-

tion of Korea NRF-2021M3F7A1082056, and the support of the Korea Institute for Advanced Study (KIAS) grant funded by the government of Korea.

-
- [1] Y. Akrami et al. (Planck), *Astron. Astrophys.* **641**, A10 (2020), [arXiv:1807.06211 \[astro-ph.CO\]](#).
- [2] J. Martin and R. Brandenberger, *Phys. Rev. D* **68**, 063513 (2003), [arXiv:hep-th/0305161](#).
- [3] X. Chen, R. Easther, and E. A. Lim, *JCAP* **04**, 010 (2008), [arXiv:0801.3295 \[astro-ph\]](#).
- [4] R. Flauger, L. McAllister, E. Pajer, A. Westphal, and G. Xu, *JCAP* **06**, 009 (2010), [arXiv:0907.2916 \[hep-th\]](#).
- [5] P. A. R. Ade et al. (Planck), *Astron. Astrophys.* **594**, A20 (2016), [arXiv:1502.02114 \[astro-ph.CO\]](#).
- [6] P. A. R. Ade et al. (Planck), *Astron. Astrophys.* **571**, A22 (2014), [arXiv:1303.5082 \[astro-ph.CO\]](#).
- [7] M. Aich, D. K. Hazra, L. Sriramkumar, and T. Souradeep, *Phys. Rev. D* **87**, 083526 (2013), [arXiv:1106.2798 \[astro-ph.CO\]](#).
- [8] J. Hamann and J. Wons, *JCAP* **03**, 036 (2022), [arXiv:2112.08571 \[astro-ph.CO\]](#).
- [9] D. K. Hazra, *JCAP* **03**, 003 (2013), [arXiv:1210.7170 \[astro-ph.CO\]](#).
- [10] F. Beutler, M. Biagetti, D. Green, A. Slosar, and B. Wallich, *Phys. Rev. Res.* **1**, 033209 (2019), [arXiv:1906.08758 \[astro-ph.CO\]](#).
- [11] M. Ballardini and F. Finelli, *JCAP* **10**, 083 (2022), [arXiv:2207.14410 \[astro-ph.CO\]](#).
- [12] T. Mergulhão, F. Beutler, and J. A. Peacock, *JCAP* **08**, 012 (2023), [arXiv:2303.13946 \[astro-ph.CO\]](#).
- [13] F. Finelli et al. (CORE), *JCAP* **04**, 016 (2018), [arXiv:1612.08270 \[astro-ph.CO\]](#).
- [14] D. K. Hazra, D. Paoletti, M. Ballardini, F. Finelli, A. Shafieloo, G. F. Smoot, and A. A. Starobinsky, *JCAP* **02**, 017 (2018), [arXiv:1710.01205 \[astro-ph.CO\]](#).
- [15] M. Ballardini, F. Finelli, C. Fedeli, and L. Moscardini, *JCAP* **10**, 041 (2016), [Erratum: *JCAP* **04**, E01 (2018)], [arXiv:1606.03747 \[astro-ph.CO\]](#).
- [16] M. Ballardini, R. Murgia, M. Baldi, F. Finelli, and M. Viel, *JCAP* **04**, 030 (2020), [arXiv:1912.12499 \[astro-ph.CO\]](#).
- [17] I. Debono, D. K. Hazra, A. Shafieloo, G. F. Smoot, and A. A. Starobinsky, *Mon. Not. Roy. Astron. Soc.* **496**, 3448 (2020), [arXiv:2003.05262 \[astro-ph.CO\]](#).
- [18] M. Ballardini et al. (Euclid), (2023), [arXiv:2309.17287 \[astro-ph.CO\]](#).
- [19] A. Antony and S. Jain, *Eur. Phys. J. C* **82**, 687 (2022), [arXiv:2110.06837 \[astro-ph.CO\]](#).
- [20] L. Covi, J. Hamann, A. Melchiorri, A. Slosar, and I. Sorbera, *Phys. Rev. D* **74**, 083509 (2006), [arXiv:astro-ph/0606452](#).
- [21] J. Hamann, L. Covi, A. Melchiorri, and A. Slosar, *Phys. Rev. D* **76**, 023503 (2007), [arXiv:astro-ph/0701380](#).
- [22] D. K. Hazra, M. Aich, R. K. Jain, L. Sriramkumar, and T. Souradeep, *JCAP* **10**, 008 (2010), [arXiv:1005.2175 \[astro-ph.CO\]](#).
- [23] A. Shafieloo and T. Souradeep, *Phys. Rev. D* **70**, 043523 (2004).
- [24] D. K. Hazra, A. Shafieloo, and T. Souradeep, *JCAP* **11**, 011 (2014), [arXiv:1406.4827 \[astro-ph.CO\]](#).
- [25] X. Chen, M. H. Namjoo, and Y. Wang, *JCAP* **1502**, 027 (2015), [arXiv:1411.2349 \[astro-ph.CO\]](#).
- [26] G. Nicholson and C. R. Contaldi, *JCAP* **07**, 011 (2009), [arXiv:0903.1106 \[astro-ph.CO\]](#).
- [27] P. Hunt and S. Sarkar, *JCAP* **12**, 052 (2015), [arXiv:1510.03338 \[astro-ph.CO\]](#).
- [28] M. Braglia, X. Chen, and D. K. Hazra, *JCAP* **06**, 005 (2021), [arXiv:2103.03025 \[astro-ph.CO\]](#).
- [29] M. Braglia, X. Chen, and D. K. Hazra, *Phys. Rev. D* **105**, 103523 (2022), [arXiv:2108.10110 \[astro-ph.CO\]](#).
- [30] D. K. Hazra, A. Antony, and A. Shafieloo, *JCAP* **08**, 063 (2022), [arXiv:2201.12000 \[astro-ph.CO\]](#).
- [31] A. Antony, F. Finelli, D. K. Hazra, and A. Shafieloo, *Phys. Rev. Lett.* **130**, 111001 (2023), [arXiv:2202.14028 \[astro-ph.CO\]](#).
- [32] J. Chluba, J. Hamann, and S. P. Patil, *Int. J. Mod. Phys. D* **24**, 1530023 (2015), [arXiv:1505.01834 \[astro-ph.CO\]](#).
- [33] E. Allys et al. (LiteBIRD), *PTEP* **2023**, 042F01 (2023), [arXiv:2202.02773 \[astro-ph.IM\]](#).
- [34] S. Aiola et al. (ACT), *JCAP* **12**, 047 (2020), [arXiv:2007.07288 \[astro-ph.CO\]](#).
- [35] L. Balkenhol et al. (SPT-3G), *Phys. Rev. D* **108**, 023510 (2023), [arXiv:2212.05642 \[astro-ph.CO\]](#).
- [36] N. Aghanim et al. (Planck), *Astron. Astrophys.* **641**, A5 (2020), [arXiv:1907.12875 \[astro-ph.CO\]](#).
- [37] See [30] for a study of different primordial features with Planck and ACT DR4 data [34]. Note however that Planck and ACT DR4 data lead to discrepant estimates for $\Omega_b h^2$ and n_s [34].
- [38] <https://pole.uchicago.edu/public/data/balkenhol22/>.
- [39] W. J. Handley, M. P. Hobson, and A. N. Lasenby, *Monthly Notices of the Royal Astronomical Society* **453**, 4385–4399 (2015).
- [40] M. Powell, Technical Report, Department of Applied Mathematics and Theoretical Physics (2009).
- [41] M. Braglia, X. Chen, and D. K. Hazra, (2021), [arXiv:2108.10110 \[astro-ph.CO\]](#).
- [42] R. Calderón, A. Shafieloo, D. K. Hazra, and W. Sohn, *JCAP* **08**, 059 (2023), [arXiv:2302.14300 \[astro-ph.CO\]](#).
- [43] Oscillations in C_ℓ^{EE} are not necessarily fit by superimposed oscillations to the curvature power spectrum which are also imprinted in C_ℓ^{TT} .
- [44] G. Franco Abellán, M. Braglia, M. Ballardini, F. Finelli, and V. Poulin, *JCAP* **12**, 017 (2023), [arXiv:2308.12345 \[astro-ph.CO\]](#).
- [45] A. R. Khalife, M. B. Zanjani, S. Galli, S. Günther, J. Lesgourgues, and K. Benabed, (2023), [arXiv:2312.09814 \[astro-ph.CO\]](#).
- [46] Oscillations in C_ℓ^{EE} are not necessarily fit by superimposed oscillations to the curvature power spectrum which are also imprinted in C_ℓ^{TT} .
- [47] P. Ade et al. (Simons Observatory), *JCAP* **02**, 056 (2019), [arXiv:1808.07445 \[astro-ph.CO\]](#).
- [48] K. Abazajian et al., *arXiv e-prints*, [arXiv:1907.04473 \(2019\)](#), [arXiv:1907.04473 \[astro-ph.IM\]](#).